Available online at www.sciencedirect.com
ScienceDirect
Journal of Sound and Vibration 302 (2007) 18–38
JOURNAL OF SOUND AND VIBRATION
www.elsevier.com/locate/jsvi

The vibroacoustics of slightly distorted cylindrical shells: A model of the acoustic input impedance

R. Picó[a,*], F. Gautier[b]

[a]*Department Física Aplicada, Esc. Politécnica Superior de Gandia, Universidad Politécnica de Valencia, Carretera Nazaret-Oliva s/n, 46700 Valencia, Spain*
[b]*Laboratoire d'Acoustique de l'Université du Maine, UMR CNRS 6613, Av. O. Messiaen, 72085 Le Mans cedex 9, France*

Received 6 December 2004; received in revised form 7 August 2006; accepted 18 October 2006
Available online 26 January 2007

Abstract

The interaction between the wall vibrations of an elastic cylindrical tube and the inner acoustic field is considered. When the tube cross section is perfectly circular, acoustic modes are coupled with structural modes having the same circumferential symmetry. Coupling between modes of different circumferential orders occur when the shell has small faults in symmetry. An analytical model using the integro-modal method is developed in order to describe these additional couplings due to shell defects. Attention is focused on the interaction between the acoustic plane mode and the ovalling shell modes. The mechanical resonance and coincidence effects between the structural and acoustical modes are found; these account for the perturbations in the input impedance induced by the wall vibrations.

1. Introduction

The vibracoustics of cylindrical ducts have been widely developed for applications in mechanical engineering such as, for example, the noise induced by industrial pipes. As a first approach, the interactions between the acoustic oscillations in the internal fluid and the vibrations of the duct can be described when considering that the cross section of the duct is perfectly circular. In practice, small faults in the circularity of the cross section always exist and such flaws in the roundness induce couplings between structural and acoustic modes which do not exist in the case where the cross section is perfectly circular. The aim of this study is to present a model which allows us to take these additional couplings, induced by geometrical defects of the shell, into account.

The final application of this study is related to musical acoustics. It concerns the problem of quantifying the effect of the wall vibrations of the body of a wind instrument on sound which is emitted [1]. To quantify this effect, a generic model of a simplified clarinet-like instrument has been developed [2,3] and constitutes the structure of the investigation presented in this paper. This simplified instrument is a cylindrical vibrating duct, acoustically excited by particle velocity distribution at the input cross section. It has been shown in Ref. [2]

*Corresponding author. Tel.: +34 962849300; fax: +34 962849309.
E-mail address: rpico@fis.upv.es (R. Picó).

0022-460X/$ - see front matter
doi:10.1016/j.jsv.2006.10.045

that the wall vibrations induce several vibroacoustic couplings: inner fluid/shell coupling, external fluid/shell coupling, and coupling induced by acoustic radiation at the open end of the tube. Descriptions of such couplings are generally complex and lead to the conclusion that, overall, these effects are very small and can be ignored since they do not induce any audible contribution. However, for some particular characteristics of the duct (that is, the particular choice of material and geometry), the wall vibration can play a significant role: in another paper [3], which employs the same notations and formalism as in this study, the acoustic input impedance of a vibrating cylindrical shell whose cross section is perfectly circular has been studied. It has been shown that the coupling between the first breathing shell mode and the plane acoustic mode can have a strong influence on the input impedance of the plane mode if both the spatial coincidence and resonance condition occur at the same frequency. These conditions can only be satisfied if the eigenfrequency of the first breathing mode is equal to that of the first acoustic antiresonance of the duct. Moreover, if the eigenfrequency of the first breathing mode is equal to that of the first acoustic resonance, a splitting of one of the resonance peaks in the impedance curve can be observed. For fixed geometrical parameters (shell length, thickness and radius), this kind of condition is only satisfied if the Young's modulus and the density of the wall material are sufficiently low, though reaching unrealistic values for the body of a wind instrument. Note that such a model of the impedance of a vibrating tube can be used to compute the time domain simulations of a clarinet's sound (see Ref. [4] for a presentation of the method and Ref. [5] for its application to a vibrating tube). Auditory tests on the musical sound allows us to determine when the wall vibration effect becomes audible.

Models of non-circular cylindrical shells have been developed in the literature. A thin shell operator is a differential operator connecting the displacement field of the mean surface of the shell to the external loads applied to the shell. A presentation of the shell theories is given in Ref. [6]. Such an operator is local and, as such, depends on the local curvatures of the medium. For a perfect cylinder, the curvatures are equal to the shell's radius in one direction and to infinity in the other direction. If the curvatures are dependent on the point chosen on the shell, then the operator has spatially dependent coefficients. In this case, the motion equation takes a complicated form, but can be solved using appropriate series expansions: [7]. The radiation of such distorted shell has been studied using this approach [8,9]. More generally, the description of complicating effects such as the influence of shell stiffening or defects in the shell introduced by added masses is discussed in Ref. [10].

The state vector method constitutes another way of computing the vibratory field of a distorted shell. This method can be applied if a description of the shell vibratory field can be given using separated variables and if the axial dependence of the field is known. This is the case for infinite or simply supported shells, in which the axial dependence of the displacement field can be assumed to be proportional to $\sin(m\pi x/L)$. Thus, the motion equation can be written as a first-order differential equation, depending on the circumferential coordinate. This kind of equation is called a state equation. A presentation of such equations to model beam, plate and shell vibrations, for example, is given in Ref. [11–13]. A numerical integration of the state equation whose parameters depend on the circumferential direction provides the solution to the problem. This method has been applied in Ref. [14–16] to shells having different types of circumferential profiles.

In this paper, we consider that the shell is slightly distorted, which corresponds to a small ovalization of the cross-section of the shell. In this case, it is possible to assume that the mode shapes and the eigenfrequencies are close to their values when the distortion parameter is equal to zero. Following Yousri and Fahy [17], such a hypothesis allows us to describe the coupling between the acoustic and structural modes of different circumferential orders within a distorted shell. The main objective of this paper is to determine the influence of the distorted shell's vibration on its input impedance matrix.

The structure of the paper is as follows: in Section 2, following the introduction, a model of the acoustic matrix impedance of a vibrating, slightly distorted shell is presented. The governing equations for the shell/internal fluid coupled problem fluid equation are given and solved within the framework of the light fluid approximation. The forced response of the system to a prescribed acoustic excitation is obtained using projections of the vibratory and acoustic fields on appropriated functional bases: the in vacuo shell modes for the structural displacement field and acoustical transverse modes for the acoustic field. The in vacuo shell modes are those of a shell having a perfectly circular cross section. The input impedance matrix is determined from the forced response of the system. In Section 3, attention is focused on the interaction of the plane acoustic mode with the first structural modes. Appropriate truncation of the functional bases is presented and coupling between the plane acoustic mode and the first structural modes (ovalling mode and breathing mode) is studied and illustrating examples are given. To conclude, a summary of the results is presented.

2. Vibroacoustic model

2.1. Statement of the problem

2.1.1. Equation of motion for a distorted shell

We consider a thin-walled cylindrical shell of length l, and thickness h. This shell is supposed to be slightly distorted: its mean radius is a and the variation of its radius is supposed to take the form:

$$r(\theta) = a(1 + \varepsilon \cos t\theta), \tag{1}$$

where $\varepsilon \ll 1$ is the non-dimensional magnitude of the distortion called the distorsion factor. The integer number t describes the type of distortion along the length of the shell (for an elliptical shell $t = 2$) and θ is the angular coordinate in the cylindrical system axis (see Fig. 1).

The shell is made from an homogeneous, isotropic material whose Young's modulus is E, its density is ρ_s and the Poisson's ratio is σ. The shell is supposed to be simply supported at both ends ($z = 0$, L).

For a perfectly circular shell (non-distorted case $\varepsilon = 0$), the motion equations of the shell in a harmonic regime can be presented in the following form (convention $e^{-j\omega t}$ is adopted, ω being the driving frequency):

$$\rho_s h(\omega_a^2 \mathscr{L} + \omega^2)\mathbf{X}(M) = -p(M)\mathbf{n} \quad \text{for } M \in S, \tag{2}$$

where ω_a is the shell ring frequency, $\mathscr{L}$ is the Donnell operator, $X(M)$ is the displacement vector of point M, belonging to the neutral surface S of the shell, $p(M)$ is the inner acoustic pressure and $\mathbf{n}$ denotes a unitary vector normal in the S surface. The displacement vector $\mathbf{X}(M)$ takes the form

$$\mathbf{X}(M) = \begin{bmatrix} u(M) & v(M) & w(M) \end{bmatrix}^{\mathrm{T}}, \tag{3}$$

where $u(M)$, $v(M)$, $w(M)$ denote longitudinal, orthoradial and radial displacements of the shell (see Fig. 1).

For a distorted shell, the equation of motion is written in the form:

$$\rho_s h\left(\tilde{\omega}_a^2 \tilde{\mathscr{L}} + \omega^2\right)\mathbf{X}\left(\tilde{M}\right) = -\tilde{p}\left(\tilde{M}\right)\mathbf{n} \quad \text{for } \tilde{M} \in \tilde{S}, \tag{4}$$

where symbol $\sim$ refers to elements related to the distorted shell. Parameter $\tilde{\omega}_a$ is defined by

$$\tilde{\omega}_a(\theta) = \frac{1}{r(\theta)}\sqrt{\frac{E}{\rho_S(1-\sigma^2)}} \tag{5}$$

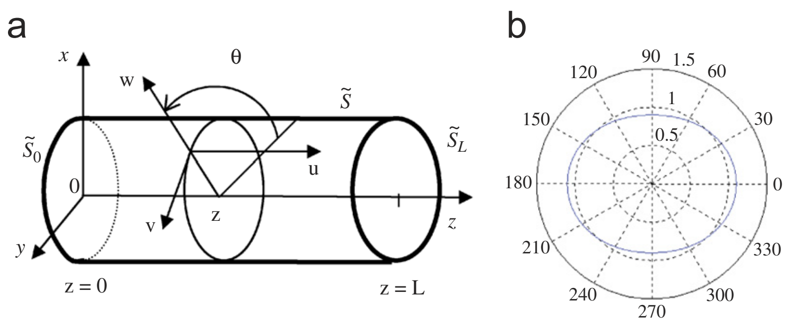

Fig. 1. Representation of the distorted shell; the axial profile and notations (a) and the cross section (b).

and coincides with the ring frequency in the case of a non-distorted shell ($r(\theta)=a$). $\tilde{\mathscr{L}}$ is the Donnell operator of the distorted shell and is defined in Eq. (6) by

$$\tilde{\mathscr{L}} = r(\theta)^2 \begin{bmatrix} \frac{\partial^2}{\partial z^2} + \frac{1-v}{2}\frac{\partial^2}{\partial s^2} & \frac{1+v}{2}\frac{\partial^2}{\partial z\,\partial s} & v\frac{\partial}{\partial z} \\ \frac{1+v}{2}\frac{\partial^2}{\partial z\,\partial s} & \frac{\partial^2}{\partial s^2} + \frac{1-v}{2}\frac{\partial^2}{\partial z^2} & \frac{\partial}{\partial s} \\ -v\frac{\partial}{\partial z} & -\frac{\partial}{\partial s} & -1-\tilde{\beta}\left(\frac{\partial}{\partial z^2}+\frac{\partial^2}{\partial s^2}\right)^2 \end{bmatrix}, \tag{6}$$

in which z is the axial coordiante, s is the curvilinear coordinate in the circumferential direction, and where the non-dimensional thickness parameter is defined by $\tilde{\beta} = h^2/(12r(\theta)^2)$. For a non-distorted shell, the curvilinear coordinate s is given by $s = a\theta$ and expression (6) coincides with the Donnell operator given in Ref. [6]. For a distorted shell, the derivatives, according to the variable s in Eq. (6), can be expressed as function of the circumferential coordinate θ. Such calculations are presented in detail in Ref. [7] and lead to complex expressions of the operator. In order to avoid to having to use these, we choose the simplified method proposed by Yousri and Fahy [17], as presented next.

Note that in relation (4), $\tilde{S}$ is the surface of the distorted shell, $\tilde{p}(\tilde{M})$ is the inner acoustic pressure at point $\tilde{M}$ belonging to $\tilde{S}$ and $\tilde{\mathbf{X}}(\tilde{M})$ is the shell displacement vector.

2.1.2. Helmholtz equation

Inside the cylindrical cavity, the acoustic pressure complies with the Helmholtz equation,

$$(\Delta + k^2)\tilde{p}(\tilde{M}) = 0, \tag{7}$$

where $k = \omega/c$ is the acoustic wavenumber. The dissipative visco-thermal effects induced by the acoustic boundary layers can be taken into account by means of the complex sound velocity c (see Ref. [2]).

Eq. (7) is associated with appropriate acoustic boundary conditions in the distorted shell surface $\tilde{S}$ and the cross sections $\tilde{S}_0$ (at $z=0$) and $\tilde{S}_L$ (at $z=L$) (see Fig. 1 for a definition of these surfaces). These surfaces are denoted without $\sim$ symbol when referring to a cylinder whose cross section is perfectly circular. On surface $\tilde{S}_0$, the normal acoustic velocity $\tilde{v}(\tilde{M})$ is supposed to be equal to a known value denoted by $\tilde{v}_{S_0}(\tilde{M})$:

$$\tilde{v}(\tilde{M}) = \tilde{v}_{S_0}(\tilde{M}), \quad \tilde{M} \in \tilde{S}_0. \tag{8}$$

The acoustic velocity distribution $\tilde{v}_{S_0}(\tilde{M})$ is considered as the excitation source of the system. On the lateral surface $\tilde{S}$, the continuity of the normal velocities of the fluid $\tilde{v}_a(\tilde{M})$ and the shell $\dot{\tilde{w}}(\tilde{M})$ is expressed as

$$\tilde{v}_a(\tilde{M}) = \dot{\tilde{w}}(\tilde{M}) \quad \text{for } \tilde{M} \in \tilde{S}. \tag{9}$$

On the surface $\tilde{S}_L$, the tube is supposed to be open and we consider that the acoustic pressure is equal to zero:

$$\tilde{p}(\tilde{M}) = 0 \quad \text{for } \tilde{M} \in \tilde{S}_L. \tag{10}$$

2.1.3. The coupled problem

The inner acoustic field $\tilde{p}(\tilde{M})$ and the wall displacement field $\tilde{\mathbf{X}}(\tilde{M})$ are the solutions to the coupled problem described by Eqs. (4) and (7), associated with the simply supported boundary conditions for the shell and with the acoustic boundary conditions (8)–(10). Both acoustic and mechanical equations underly the vibroacoustic nature of the coupled problem. The resolution method consists of determining the forced response of the problem to the known velocity distribution $\tilde{v}_{S_0}(\tilde{M})$. This response provides the input acoustic impedance of the distorted cylinder with vibrating wall, which is the quantity being searched.

2.2. Resolution method

2.2.1. Expansion of the shell displacement field on a functional basis

The distorted shell displacement field is expanded in the in vacuo shell modes of a shell having a perfectly circular cross section. These modes take the form

$$\mathbf{\Phi}_\mu = \begin{bmatrix} \Phi_{1\mu} \\ \Phi_{2\mu} \\ \Phi_{3\mu} \end{bmatrix} = \begin{bmatrix} U_\mu \cos(q\pi z/l)\sin(m\theta + s\pi/2) \\ V_\mu \sin(q\pi z/l)\cos(m\theta + s\pi/2) \\ \sin(q\pi z/l)\sin(m\theta + s\pi/2) \end{bmatrix}, \tag{11}$$

where $\mu = (m, q, s)$ is a set of 3 modal indices: m is the circumferential index, q is the axial index and s is the symmetry index. There is a fourth modal index, j, called type index, but for thin shells, usually only the smaller solution, corresponding to $j = 1$ produces a predominant radial mode. For this study, the value $j = 1$ is the only one taken into account. We disregard the other two ($j = 2$ and 3) due to the fact that the corresponding eigenfrequencies are in the ultrasound-range frequency. Thus, from now on, the structural modal indices will be considered as the triplet: $\mu = (m, q, s)$.

The modal amplitudes U_μ and V_μ are determined using the shell motion equation. The modes $\mathbf{\Phi}_\mu$ constitute a functional basis on which the vibratory field can be expanded [10]. We assume that

$$\tilde{\mathbf{X}}(\tilde{M}) = \sum_\mu \tilde{A}_\mu \mathbf{\Phi}_\mu(\tilde{M}), \tag{12}$$

where $\tilde{A}_\mu$ are the unknown modal amplitudes. Such a choice allows us to avoid the computation of the in vacuo modes of the distorted shell. Moreover, since the ovalization parameter ε is small compared to 1, it also seems reasonable to suppose that the mode shapes of the distorted shell $\tilde{\mathbf{\Phi}}_\mu$ (associated with the eigenfrequency $\tilde{\omega}_\mu$) are similar to the mode shapes of the non-distorted shell $\mathbf{\Phi}_\mu$ (associated with the eigenfrequency ω_μ). The first important assumption of the model is expressed as

$$\tilde{\mathbf{\Phi}}_\mu \cong \mathbf{\Phi}_\mu. \tag{13}$$

Assumption (13) implies that the shape of the distorted shell is very close to the shape of the non-distorted shell. For a non distorted shell, the mode defined by $\mu = (m, q, 0)$ (having the modal symmetry index $s = 0$) has the same axial dependence as the mode $\mu = (m, q, 1)$, (having the modal symmetry indices $s = 1$) but is rotated by angle $2\pi/m$. These two types of modes are degenerate since their eigenfrequencies are exactly the same. The main difference between the modal basis of the distorted and the non-distorted shell remains in the fact that the eigenfrequencies of the circular shell are split by the defect in the shell. The frequency shift induced by this splitting is supposed to be small, but even if it is observable, it does not introduce any additional coupling effect. Thus, this frequency shift is ignored and results in

$$\tilde{\omega}_\mu \cong \omega_\mu \tag{14}$$

2.2.2. Projection of the equation of motion

Dividing Eq. (4) by $\tilde{\omega}_a^2$ and projecting it on mode $\mathbf{\Phi}_{\mu'}^{\mathrm{T}}$ leads to

$$\sum_\mu \tilde{A}_\mu \left\{ \int_S \rho h \mathbf{\Phi}_{\mu'}^{\mathrm{T}} \tilde{L} \mathbf{\Phi}_\mu \, \mathrm{d}S + \int_S \rho h \mathbf{\Phi}_{\mu'}^{\mathrm{T}} \mathbf{\Phi}_\mu \frac{\omega^2}{\tilde{\omega}_a^2} \, \mathrm{d}S \right\} = -\int_S \frac{\mathbf{\Phi}_{\mu'}^{\mathrm{T}} \tilde{p} \mathbf{n}}{\tilde{\omega}_a^2}. \tag{15}$$

The modes of the distorted shell $\tilde{\mathbf{\Phi}}_\mu$ associated with the eigenfrequency $\tilde{\omega}_\mu$ comply with the homogeneous equation of motion:

$$\tilde{\omega}_a^2 \tilde{L} \tilde{\mathbf{\Phi}}_\mu + \tilde{\omega}_\mu^2 \tilde{\mathbf{\Phi}}_\mu = 0. \tag{16}$$

Considering assumptions (13) and (14), Eq. (16) leads to

$$\tilde{L} \mathbf{\Phi}_\mu \cong -\frac{\omega_\mu^2}{\tilde{\omega}_a^2} \mathbf{\Phi}_\mu. \tag{17}$$

With this approximation, the shell motion Eq. (15) can be written as

$$\sum_{\mu} \tilde{A}_{\mu} \left\{ \int_S \rho h \mathbf{\Phi}_{\mu'}^{\mathrm{T}} \frac{\omega^2 - \omega_{\mu}^2}{\tilde{\omega}_a^2} \mathbf{\Phi}_{\mu} \, \mathrm{d}S \right\} \cong - \int_S \frac{\mathbf{\Phi}_{\mu'}^{\mathrm{T}} \tilde{p} \mathbf{n}}{\tilde{\omega}_a^2} \, \mathrm{d}S. \tag{18}$$

It must be pointed out that the dependency of $\tilde{\omega}_a = \tilde{\omega}_a(\theta)$ is linked to the distortion of the shell. As a second important assumption, we ignore this dependency in the left-hand term of Eq. (18) which is written as

$$\sum_{\mu} \tilde{A}_{\mu} \frac{\omega^2 - \omega_{\mu}^2}{\omega_a^2} \int_S \rho h \mathbf{\Phi}_{\mu'}^{\mathrm{T}} \mathbf{\Phi}_{\mu} \, \mathrm{d}S \cong - \int_S \frac{\mathbf{\Phi}_{\mu'}^{\mathrm{T}} \tilde{p} \mathbf{n}}{\tilde{\omega}_a^2} \, \mathrm{d}S. \tag{19}$$

The modes $\mathbf{\Phi}_{\mu}$ are normal modes and adhere to the orthogonality relationship

$$\int_S \rho h \mathbf{\Phi}_{\mu'}^{\mathrm{T}} \mathbf{\Phi}_{\mu} \, \mathrm{d}S = m_{\mu} \delta_{\mu\mu'}, \tag{20}$$

where the modal mass m_{μ} of the mode $\mathbf{\Phi}_{\mu}$ is defined as

$$m_{\mu} = \int_S \rho \mathbf{\Phi}_{\mu}^{\mathrm{T}} \mathbf{\Phi}_{\mu} \, \mathrm{d}S \tag{21}$$

and where $\delta_{\mu\mu'}$ denotes the Kronecker symbol. Using the orthogonality relationship (20) and the series expansion,

$$\frac{1}{\tilde{\omega}_a^2} \cong \frac{1 + 2\varepsilon \cos(t\theta)}{\omega_a^2}, \tag{22}$$

relation (19) takes the form

$$m_{\mu'} \left(\omega^2 - \omega_{\mu'}^2 \right) \tilde{A}_{\mu'} \cong - \int_S (1 + 2\varepsilon \cos(t\theta)) \tilde{p}(M) \mathbf{\Phi}_{\mu'}^{\mathrm{T}}(M) \mathbf{n} \, \mathrm{d}S. \tag{23}$$

The shell mechanical damping can be taken into account by introducing a structural damping term (involving $\eta_{\mu'}$ parameter) for each strutural mode μ' into Eq. (23):

$$m_{\mu'} \left(\omega^2 - \omega_{\mu'}^2 (1 - \mathrm{j}\eta_{\mu'}) \right) \tilde{A}_{\mu'} \cong - \int_S (1 + 2\varepsilon \cos(t\theta)) \tilde{p}(M) \mathbf{\Phi}_{\mu'}^{\mathrm{T}}(M) \mathbf{n} \, \mathrm{d}S. \tag{24}$$

The above equation (24) shows that coupling between the plane acoustic wave mode and non-axisymmetric structural modes is permitted by the defects, since, in this case, the right-hand term of the equation does not equal zero. This equation is equivalent to that presented by Yousri and Fahy in Ref. [17], but using the notations given in this work.

2.2.3. *Determination of the inner acoustic field*

In order to compute the forced response of the shell, the acoustic pressure $\tilde{p}(\tilde{M})$ acting on the shell has to be replaced in the motion Eq. (24) by its expression, according to the displacement field of the shell. Such an expression is obtained using the integral representation [18]. Considering that the surfaces S and $\tilde{S}$ are the same, we can write the inner acoustic pressure as

$$\tilde{p}(\tilde{M}) \cong p(M) = \int_{S_0, S, S_l} [G(M, M_0) \partial_n P(M) - p(M) \partial_n G(M, M_0)] \, \mathrm{d}S, \tag{25}$$

The Green's function

$$G(M, M_0) = \frac{\mathrm{j}}{2} \sum_{\alpha} \frac{\Psi_{\alpha}(M, \theta) \Psi_{\alpha}^{*}(M_0, \theta)}{k_{mn}} \, \mathrm{e}^{\mathrm{j}k_{mn}|z - z_0|}, \tag{26}$$

is the Green's function of the infinite cylinder satisfying the Neumann boundary conditions in the S surface of the wall. The acoustic modes $\Psi_{\alpha}(r, \theta)$ are those of a non-distorted cross section and are given by Gautier and

Tahani [2], Morse and Ingard [19] and Picó et al. [3] as

$$\Psi_\alpha(r,\theta) = J_m(k_{Wmn} r)\,\sin\big(m\theta + s\pi/2\big)/\Lambda_\alpha, \tag{27}$$

where the normalization factor Λ_α is

$$\Lambda_\alpha^2 = \frac{\pi a^2}{\varepsilon_m}\big(1-\gamma_{mn}^2\big)J_m^2(k_{Wmn}a), \quad \text{with } \gamma_{mn}^2 = \begin{cases} 0, & m=0, \\ m^2/(k_{Wmn}a)^2, & m>0. \end{cases} \tag{28, 29}$$

The longitudinal eigenvalue k_{mn} is given by $k_{mn}^2 = k^2 - k_{Wmn}^2$ ($\mathrm{Re}(k_{mn})\geqslant 0$, $\mathrm{Im}(k_{mn})\geqslant 0$), the radial eigenvalue k_{Wmn} by $J'_m(k_{Wmn}a) = 0$ ($k_{Wmn}\geqslant 0, n\geqslant 0$) and ε_m is the Neumann factor ($\varepsilon_m = 1$ if $m=0$, $\varepsilon_m = 2$ if $m>0$). The triplet $\alpha = (m, n, s)$ is used to group the 3 indices m, n, s which are the circumferential, radial and symmetry modals, respectively. Note that in expression (25), it has been assumed that $\tilde{\Psi}_\alpha(r,\theta) = \Psi_\alpha(r,\theta)$. This is justified by the fact that the ovalization parameter is supposed to be very small. The modes $\Psi_\alpha(r,\theta)$ play the role of a functional basis upon which the acoustical field can be expanded.

Using relations (8)–(10), the general expression of the field can be expressed as the superposition of travelling waves propagating in opposite directions with amplitudes according to z:

$$\tilde{p}(r,\theta,z) = \sum_{\alpha=(m,n,s)} \Big[\{\tilde{B}_\alpha + \tilde{D}_\alpha^+(z)\}\,\mathrm{e}^{\mathrm{j}k_{mn}z} + \{\tilde{B}_\alpha^- + \tilde{D}_\alpha^-(z)\}\,\mathrm{e}^{\mathrm{j}k_{mn}(1-z)}\Big]\Psi_\alpha(r,\theta). \tag{30}$$

In relation (30), we retain the notation $\sim$ since this expression takes into account the vibration of the distorted shell through the amplitude terms $\tilde{D}_\alpha^+(z)$, $\tilde{D}_\alpha^-(z)$, $\tilde{B}_\alpha^+$, $\tilde{B}_\alpha^-$. These are defined by

$$\tilde{D}_\alpha^+(z) = \frac{-\rho}{2k_{mn}}\int_0^{2\pi}\int_0^z \dot{\tilde{w}}(z,\theta)\mathrm{e}^{-\mathrm{j}k_{mn}z_0}\Psi_\alpha(a,\theta) r\,\mathrm{d}\theta, \tag{31}$$

$$\tilde{D}_\alpha^-(z) = \frac{-\rho}{2k_{mn}}\int_0^{2\pi}\int_z^l \dot{\tilde{w}}(z,\theta)\mathrm{e}^{-\mathrm{j}k_{mn}(z_0-l)}\Psi_\alpha(a,\theta) r\,\mathrm{d}\theta \tag{32}$$

and

$$\tilde{B}_\alpha^+ = \frac{1}{1+\mathrm{e}^{2\mathrm{j}k_{mn}l}}\Big[\big\langle \bar{v}_{S_0}|\Psi_\alpha(r,\theta)\big\rangle_{S_0} + \tilde{D}_\alpha^-(0)\,\mathrm{e}^{\mathrm{j}k_{mn}l} - \tilde{D}_\alpha^+(l)\mathrm{e}^{2\mathrm{j}k_{mn}l}\Big], \tag{33}$$

$$\tilde{B}_\alpha^- = \frac{1}{1+\mathrm{e}^{2\mathrm{j}k_{mn}l}}\Big[-\big\langle \bar{v}_{S_0}|\Psi_\alpha(r,\theta)\big\rangle_{S_0} - \tilde{D}_\alpha^-(0)\mathrm{e}^{2\mathrm{j}k_{mn}l} - \tilde{D}_\alpha^+(l)\mathrm{e}^{\mathrm{j}k_{mn}l}\Big]. \tag{34}$$

The inner product $\langle \cdot | \cdot \rangle$ used in Eq. (33) and (34) is defined by the relationship $\langle f|g\rangle = \int_S fg\,\mathrm{d}S$.

2.2.4. Light fluid approximation

The light fluid approximation is considered for the determination of the acoustic pressure $\tilde{p}$, which is involved in the shell motion Eq. (24). The physical meaning of this approximation is schematically explained in Fig. 2. The block diagram describes the shell/inner fluid interaction when considering the approximation of light fluid in the 5 steps. Several relations, using matrix relations which are introduced later, are indicated in this figure.

1. The tube is excited at the entrance in cross section S_0 by an imposed velocity of $\bar{v}_{S_0}(\tilde{M})$.
2. An acoustic pressure field termed p_a is generated in the tube by the excitation. At this stage, the wall vibration effect on the inner pressure field is not considered and the pressure p_a is called 'blocked pressure'. This blocked pressure p_a is noted without $\sim$ because it does not depend on the wall distortion.
3. The distorted shell displacement field $\tilde{\mathbf{X}}$ is induced by the inner acoustic field p_a. Even if p_a is calculated without accounting for the shell distortion, $\tilde{X}$ is notated with $\sim$ because the displacement field depends on the distortion of the shell. Part of the acoustic energy of the air column is transformed into the vibrating energy of the shell.

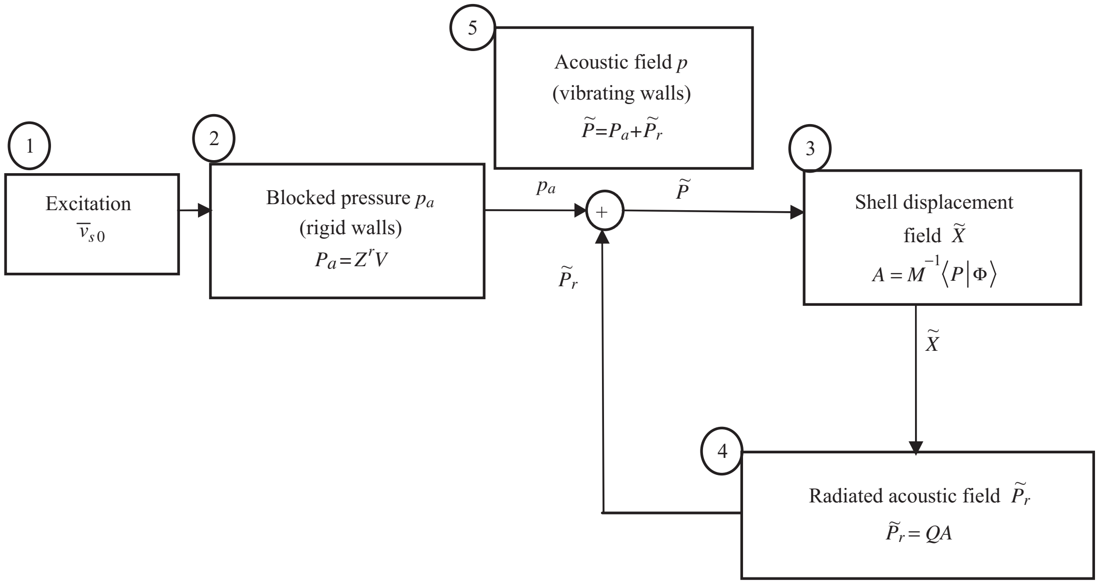

Fig. 2. Block diagram describing the shell/inner fluid interaction. Acoustic pressure P_a refers to the blocked pressure or pressure calculated without wall vibration. Acoustic pressure $\tilde{P}_r$ refers to the inner pressure radiated by the shell.

4. In turn, the wall vibration generates an additional acoustic radiated field $\tilde{p}_r$ in the resonator.
5. The resulting inner acoustic field of a vibrating shell $\tilde{p}$ is the sum of two contributions: The acoustic field arising from the acoustic excitation of the tube at the entrance (p_a) and the radiated field generated by the wall vibration effect ($\tilde{p}_r$).

Such an approach can be used to compute the solution to the coupled problem employing successive approximations of the fields: the pressure $\tilde{p} = p_a + \tilde{p}_r$ being obtained, in turn can be used to calculate the shell response. The acoustic field radiating from the shell can then be computed and constitutes an approximation of the acoustic field of a higher order. Such a computation can be repeated and the complete procedure can be organised in an iterative manner in order to converge with the solution for the coupled problem. A formulation for this iterative method is given in Ref. [20].

In the light fluid approximation, wall vibration is supposed to be generated by the blocked acoustic pressure p_a and not by the radiated field engendered by the walls $\tilde{p} = p_a + \tilde{p}_r$. This corresponds to the first step of the iterative method mentioned above. Such an approximation is equivalent to ignoring the effect of the internal radiation impedance of the shell.

Assuming the light fluid approximation, the inner acoustic pressure which is present in the right-hand term of the equation of motion (24) is supposed to be p_a and is computed by ignoring the wall vibration. This is equivalent to setting coefficients $\tilde{D}^+_\alpha(z)$, $\tilde{D}^-_\alpha(z)$ to zero in relation (30):

$$p_a(r,\theta,z) = \sum_{\alpha=(m,n,s)} \left[B^+_\alpha \mathrm{e}^{\mathrm{j}k_{mn}z} + B^-_\alpha \mathrm{e}^{\mathrm{j}k_{mn}(l-z)}\right] \Psi_\alpha(r,\theta). \tag{35}$$

The amplitudes B^+_α, B^-_α are expressed as the projection of the velocity distribution constituting the excitation field in the acoustical modes $\Psi_\alpha(r,\theta)$:

$$B^+_\alpha = \frac{1}{1+\mathrm{e}^{2\mathrm{j}k_{mn}l}} \left\langle \bar{v}_{S_0} | \Psi_\alpha(r,\theta) \right\rangle_{S_0}, \tag{36}$$

$$B^-_\alpha = \frac{1}{1+\mathrm{e}^{2\mathrm{j}k_{mn}l}} \left\langle \bar{v}_{S_0} | \Psi_\alpha(r,\theta) \right\rangle_{S_0}. \tag{37}$$

2.2.5. Modal coupling induced by shell distortion

Once the acoustic pressure is obtained as a multimodal expansion, the coupling between the acoustic modes and the structural modes can be evaluated. For this purpose, the expression of the internal pressure (35) is replaced in the right-hand term of the shell motion Eq. (24). It is established that the coupling term $\int_S \tilde{p}\mathbf{\Phi}_{\mu'}^{\mathrm{T}}\mathbf{n}(1+2\varepsilon\cos(t\theta))\,\mathrm{d}S$ is the sum of two contributions I_n and I_d

$$\int_S \tilde{p}\mathbf{\Phi}_{\mu'}^{\mathrm{T}}\mathbf{n}(1+2\varepsilon\cos(t\theta))\,\mathrm{d}S = \int_S p_a\mathbf{\Phi}_{\mu'}^{\mathrm{T}}\mathbf{n}(1+2\varepsilon\cos(t\theta))\,\mathrm{d}S = I_n + I_d, \tag{38}$$

where

$$\begin{aligned} I_n &= \int_S p_a\mathbf{\Phi}_{\mu'}^{\mathrm{T}}\mathbf{n}\,\mathrm{d}S \\ &= \sum_\alpha \frac{\mathrm{j}\rho\omega}{k_{mn}}\frac{1}{a}\sqrt{\frac{\varepsilon_m}{\pi}}\frac{1}{\sqrt{1-\gamma_{mn}^2}}\frac{q'\pi}{l}\frac{\tan(k_{mn}l)}{k_{mn}^2-\left(q'\pi/l\right)^2}\left\langle v_{S_0}|\Psi_\alpha\right\rangle \mathrm{i}_{\alpha\mu'} \end{aligned} \tag{39}$$

and

$$\begin{aligned} I_d &= 2\varepsilon\int_S p_a\mathbf{\Phi}_{\mu'}^{\mathrm{T}}\mathbf{n}\cos(t\theta)\,\mathrm{d}S \\ &= \varepsilon\sum_\alpha \frac{\mathrm{j}\rho\omega}{k_{mn}}\frac{1}{a}\sqrt{\frac{\varepsilon_m}{\pi}}\frac{1}{\sqrt{1-\gamma_{mn}^2}}\frac{q'\pi}{l}\frac{\tan(k_{mn}l)}{k_{mn}^2-\left(q'\pi/l\right)^2}\left\langle v_{S_0}|\Psi_\alpha\right\rangle I_{\alpha\mu'}. \end{aligned} \tag{40}$$

In these relations (39) and (40), the implicit notation $\mu' = (m', q', s')$ and $\alpha = (m, n, s)$ is assumed. The first contribution I_n is independent of the distortion parameter ε and refers to the fluid/shell coupling of a non-distorted shell. The term $i_{\alpha\mu'}$, which is present in the sum (39), is given by

$$i_{\alpha\mu'} = \int_0^{2\pi}\sin\left(m\theta+s\pi/2\right)\,\sin\left(m'\theta+s'\pi/2\right)\mathrm{d}\theta = \frac{2\pi}{\varepsilon_m}(1-\delta_{m0}\delta_{s0})\delta_{mm'}\delta_{ss'}. \tag{41}$$

As shown in expression (41), modal coupling between different family modes is forbidden by the term $\delta_{mm'}\delta_{ss'}$. In particular, this implies that the plane mode ($m=0$) is uncoupled to structural modes of order $m' \neq 0$.

The second contribution I_d describes the specific coupling induced by the defects in the shell and vanishes in the case of the non-distorted shell. The term $I_{\alpha\mu'}$, present in the expression of I_d, is given by

$$I_{\alpha\mu'} = \int_0^{2\pi}\sin\left(m\theta+s\pi/2\right)\sin\left(m'\theta+s'\pi/2\right)\,\cos(t\theta)\,\mathrm{d}\theta. \tag{42}$$

It depends on the modal numbers m, m', s, s' and on the parameter t relating to the type of circumferential defect of the shell. Rather than writing out the long expression for $I_{\alpha\mu'}$ in the general case, we give its value in the special case $t=2$. Here, it can be shown that integral (42) is non-null only when

$$m + m' = 2 \tag{43}$$

and if condition (43) is satisfied, this results in

$$I_{\alpha\mu'} = \frac{\pi(-1)^{\delta_{mm'}}}{1+\delta_{mm'}}(1-\delta_{m0}\delta_{s0})(1-\delta_{m'0}\delta_{s'0})\delta_{ss'}. \tag{44}$$

Indices m and m' being natural numbers, only three couples of values provide non-null values of $I_{\alpha\mu'}$: ($m=0$, $m'=2$), ($m=2$, $m'=0$) and ($m=1$, $m'=1$). Expression (44) provides useful information concerning the modal couplings. $I_{\alpha\mu'}$ is null if symmetry indices s and s' are different, or if ($s=0$ and $m=0$) or if ($s'=0$ and $m'=0$). The distortion of the shell introduces the presence of an additional coupling between acoustical and structural modes of different circumferential indices: the plane acoustic mode is coupled to the ovalling modes of the shell ($m=0$, $m'=2$). In addition, the breathing modes are coupled to the second-order acoustic modes ($m=2$, $m'=0$). Finally, the bending modes are coupled to the first order acoustic modes ($m=1$, $m'=1$).

The main conclusion of this paragraph is the expression of the coupling term (38), which is involved in the shell motion Eq. (24). The integrals $i_{\alpha\mu'}$ and $I_{\alpha\mu'}$, given by Eqs. (41) and (44), provide the necessary conditions in the modal indices to permit modal coupling. It is shown that couplings between acoustic modes and structural modes having circumferential indices are permitted by the distortion in the shell.

2.3. Determination of the input impedance matrix

Once the modal coupling is evaluated, the expression of the input acoustic impedance can be obtained. For this purpose, a matrix notation will be used (see Appendix A) in order to represent the multimodal formulation. In this notation, Eq. (24) can be written as

$$\mathbf{MA} = \mathbf{EV}, \tag{45}$$

where $\mathbf{M}$ is a diagonal matrix whose elements consist of the expression $m_{\mu'}(-\omega^2 + \omega_{\mu'}^2(1 - \mathrm{j}\eta_{\mu'}))$ calculated for each modal index of the structural modal basis. In Eq. (45), the amplitude vector $\mathbf{V}$ for the acoustic velocity is given since the velocity is prescribed for the input surface S_0. Vector $\mathbf{A}$ represents the amplitude of the wall vibrations and matrix $\mathbf{E}$ (see Appendix A) the shell/fluid coupling. This coupling can be separated into two contributions (non-distorted coupling and distorted coupling):

$$\mathbf{E} = \mathbf{E}_n + \varepsilon \mathbf{E}_\mathrm{d}. \tag{46}$$

Both vector $\mathbf{A}$ and matrix $\mathbf{E}$ can be deduced from Eq. (24). For a particular pattern of wall vibration amplitude generated by the acoustic field p_a, the inner acoustic pressure radiated $\tilde{p}_r$ by the shell is shown in the form of a multimodal acoustic expansion given by Eq. (30). By projecting the inner pressure onto a particular mode Ψ_α of the acoustic basis on surface S_0, we obtain

$$\langle \tilde{p}(\tilde{M}) | \Psi_\alpha \rangle_{S_0} = B_\alpha^+ + \tilde{D}_\alpha^+(0) + \left[B_\alpha^- + \tilde{D}_\alpha^-(0) \right] \mathrm{e}^{\mathrm{j}k_{mn}l}. \tag{47}$$

Note that, again, the light fluid approximation has been used when writing B_α^+ (and B_α^+) instead of $\tilde{B}_\alpha^+$ (and $\tilde{B}_\alpha^-$).

Using the matrix notation given in Appendix A, the expression of the projections of the inner pressure on the transverse acoustic modes (47) can be expressed in the form:

$$\mathbf{P} = \mathbf{Z}^r\mathbf{V} + \mathbf{QA}, \tag{48}$$

where matrix $\mathbf{Q}$ can be deduced from Eqs. (31)–(34) and (47) and expressed in the matrix form as (see Appendix A for the matrix notations)

$$\mathbf{Q} = \mathbf{Q}_n + \varepsilon \mathbf{Q}_d. \tag{49}$$

The impedance matrix $\mathbf{Z}^r$ in Eq. (46) is the impedance matrix of a rigid cylindrical duct. Indeed, for a rigid wall, we have $\mathbf{A} = \mathbf{0}$ and, therefore, in this case, we simply have $\mathbf{P} = \mathbf{Z}^r\mathbf{V}$. Eqs. (45) and (48) provide an expression of the acoustic input impedance of the distorted shell:

$$\mathbf{Z} = \mathbf{Z}^r + (\mathbf{Q}_n + \varepsilon \mathbf{Q}_d)\mathbf{M}^{-1}(\mathbf{E}_n + \varepsilon \mathbf{E}_d). \tag{50}$$

By expanding this Eq. (50), we obtain an expression of the acoustic input impedance of a slightly distorted vibrating shell

$$\mathbf{Z} = \mathbf{Z}^r \Big(\mathbf{I} + \mathbf{Z}^{r-1}\mathbf{Q}_n\mathbf{M}^{-1}\mathbf{E}_n + \varepsilon \mathbf{Z}^{r-1}(\mathbf{Q}_d\mathbf{M}^{-1}\mathbf{E}_n + \mathbf{Q}_n\mathbf{M}^{-1}\mathbf{E}_d) + \varepsilon^2 \mathbf{Z}^{r-1}\mathbf{Q}_d\mathbf{M}^{-1}\mathbf{E}_d \Big). \tag{51}$$

3. Wall distortion influence on the acoustic input impedance

3.1. Truncations of the functional basis

The functional basis used to expand the shell displacement field is constituted by the shell modes whose cross section is perfectly circular. It has been established that the eigenfrequencies of such a shell are not ordered in the same way as the modal indices. In particular, the fundamental frequency (that is the lowest

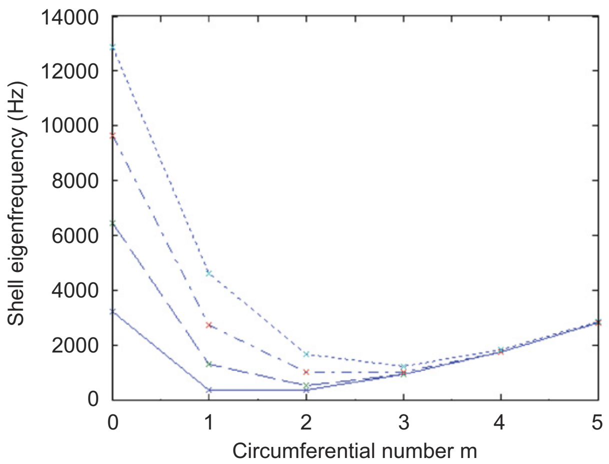

Fig. 3. Shell eigenfrequencies of a steel shell ($E = 210$ GPa, $\sigma = 0.28$, $\rho = 7800\,\mathrm{kg/m^3}$, $a = 14.25$ mm, $L = 0.5$ m, $h = 0.5$ mm) for different circumferential modal index m and axial modal index q (——— $q = 0$, —— $q = 1$, –·–· $q = 2$, ... $q = 3$). The eigenfrequencies of bending modes ($m = 1$) and ovalling modes ($m = 2$) are lower in frequency than those for the breathing modes ($m = 0$).

eigenfrequency) does not generally correspond to the first breathing mode, but to a mode associated with a higher circumferential index. A discussion concerning the value of the lowest eigenfrequency (also called fundamental frequency) of a shell is given in Ref. [21]. This point is illustrated in Fig. 3: the dispersion curves and eigenfrequencies modes of a shell made of steel (the characteristics are given in Table 2) are presented depending on the values of the modal indices q and m. Using Fig. 3, the lowest eigenfrequency is found for $m = 2$, $q = 1$ corresponding to the first ovalling mode.

Acoustic and shell modal indices are represented by $\alpha = (m, n, s)$ and $\mu' = (m', q', s')$, respectively. The simplest modal truncation, rendering the effect of the shell distortion, will be considered. Thus, the circumferential indices m and m' vary from 0 to 2 in order to take into account the coupling between different shell family modes. The symmetry indices s and s' vary from 0 to 1 to allow for the asymmetry of the shell. Indices q' and n take the first value of the truncation ($q' = 1$ and $n = 0$). With this choice of modal indices, the set of modes include six acoustic modes and six shell modes represented in Figs. 4 and 5: values of α are (0, 0, 0), (0, 0, 1), (1, 0, 0), (1, 0, 1), (2, 0, 0), (2, 0, 1) and values of μ' are (0, 1, 0), (0, 1, 1), (1, 1, 0), (1, 1, 1), (2, 1, 0), (2, 1, 1).

3.2. The interaction between the plane acoustic mode and the first ovalling shell modes: expression of the correction factor for the input impedance

The influence of the angular distortion of the shell on the acoustic behaviour of the tube is considered in the case of the particular truncation defined in Section 3.1. The matrices **Q**, **M** and **E** are presented in Appendix B. The factor correction of the plane mode can be expressed as

$$Z_{(0,0,1)(0,0,1)} = Z^r_{(0,0,1)(0,0,1)}\left(1 + C_{(0,0,1)(0,0,1)}\right), \tag{52}$$

where

$$C_{(0,0,1)(0,0,1)} = C_n + C_d, \tag{53}$$

$$\begin{aligned} C_n &= Z^{-1}_{(0,0,1)(0,0,1)} Q_{(0,0,1)(0,1,1)} M^{-1}_{(0,1,1)(0,1,1)} E_{(0,1,1)(0,0,1)} \\ &= \frac{\pi\rho c}{m_{(0,1,1)}}\left(\frac{\pi}{l}\right)^2 \frac{\omega\,\tan(\omega l/c)}{\left[(\omega/c)^2 - (\pi/l)^2\right]^2\left[\omega^2 - \omega^2_{(0,1,1)}\left(1 - \mathrm{j}\eta_{(0,1,1)}\right)\right]}(2-\varepsilon)^2 \end{aligned} \tag{54}$$

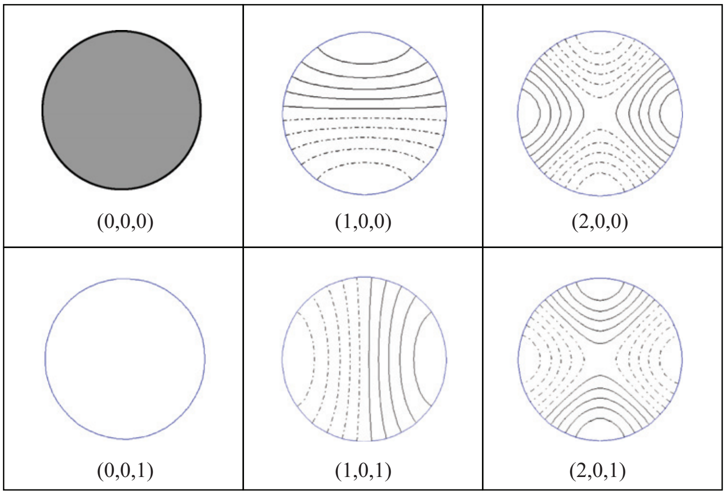

Fig. 4. Representation of the first transverse acoustic modes used for the numerical investigation presented in Section 3.3. Each mode is referred by the set of modal indices, $\alpha = (m, n, s)$ where m is the circumferential index ($m = 0, 1, 2$), n the radial index ($n = 0$), and s the index of symmetry ($s = 0, 1$).

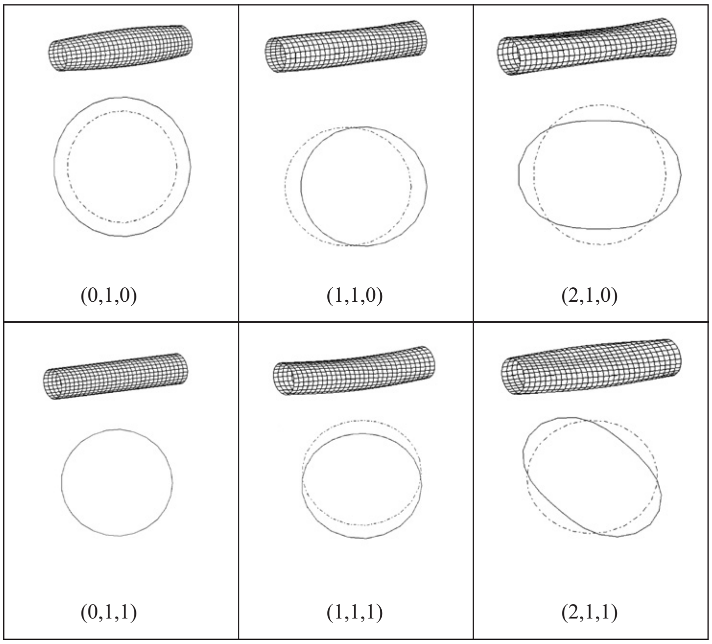

Fig. 5. Representation of the first structural modes used for the numerical investigation presented in Section 3.3 Each mode is referenced by the set of modal indices, $\mu = (m, q, s)$ where m denotes the circumferential index ($m = 0, 1, 2$), q denotes the axial index ($q = 1$) and s is the index of symmetry ($s = 0, 1$).

and

$$\begin{aligned} C_d &= Z^{-1}_{(0,0,1)(0,0,1)} Q_{(0,0,1)(2,1,1)} M^{-1}_{(2,1,1)(2,1,1)} E_{(2,1,1)(0,0,1)} \\ &= 4\varepsilon^2 \frac{\pi\rho c}{m_{(2,1,1)}} \left(\frac{\pi}{al}\right)^2 \frac{\omega \tan(\omega l/c)}{\left[(\omega/c)^2 - (\pi/l)^2\right]^2 \left[\omega^2 - \omega^2_{(2,1,1)}\left(1 - \mathrm{j}\eta_{(2,1,1)}\right)\right]}. \end{aligned} \tag{55}$$

As such, the correction factor of the input acoustic impedance of the plane mode given by Eq. (52) can be interpreted as the sum of two contributions: the first one represents the fluid/shell coupling corresponding to a shell with a perfectly cylindrical cross-section C_n. As presented in Ref. [3], this term tends towards a maximum when a mechanical resonance is reached. This mechanical resonance is characterized by the eigenfrequency of the first breathing mode ($\omega_{(0,\ 1,\ 1)}$), and its structural damping coefficient ($\eta_{(0,\ 1,\ 1)}$). The second contribution C_d is an additional term relating to the coupling of the first ovalling mode (2, 1, 1) and the plane acoustic mode. This term is proportional to the distortion of the shell ε and tends towards a maximum when a mechanical resonance for the ovalling mode is reached: this mechanical resonance is characterized by the eigenfrequency of the first ovalling mode ($\omega_{(2,\ 1,\ 1)}$), and its structural damping coefficient ($\eta_{(2,\ 1,\ 1)}$).

It can be seen from Eq. (52) that the input acoustic impedance of the plane mode can be drastically perturbed by the wall vibration if the correction factor $C_{(0,\ 0,\ 1)(0,\ 0,\ 1)}$ is significant when compared to unity. As presented in Ref. [3], three conditions lead to large values for both the correction factors C_n and C_d in Eqs. (54) and (55) and three phenomena underpin this singular behaviour: a spatial coincidence effect, mechanical resonances and acoustic resonances. If two of these phenomena simultaneously occur, the perturbation effect becomes significant and the acoustic resonances and antiresonances of the tube can be altered significantly.

3.3. Analysis of the variation correction factor versus frequency

The correction factor of the input acoustic impedance is analysed in this paragraph in order to establish and identify the contribution of the distortion of the shell to the acoustic response of the tube. The geometrical features of the shell which are used for the numerical applications are: length $l = 0.5$ m, radius $a = 14.25$ mm, thickness $h = 0.35$ mm, and the distortion parameter is fixed at $\varepsilon = 0.05$. Fig. 6 represents the two contributions made by the correction factor against the frequency of a shell made of steel: the non-distorted C_n and the distorted C_d correction factor. It can be seen that, at low frequencies, the coupling resulting from the shell distortion is more important than that resulting from the non-distorted contribution. The elliptical distortion of the cross-section of the shell permits the coupling between the plane mode and the first ovalling shell mode. The eigenfrequency of the first breathing shell mode ($f_{\mathrm{Rb1}} = 3243$ Hz) can be identified as a peak in

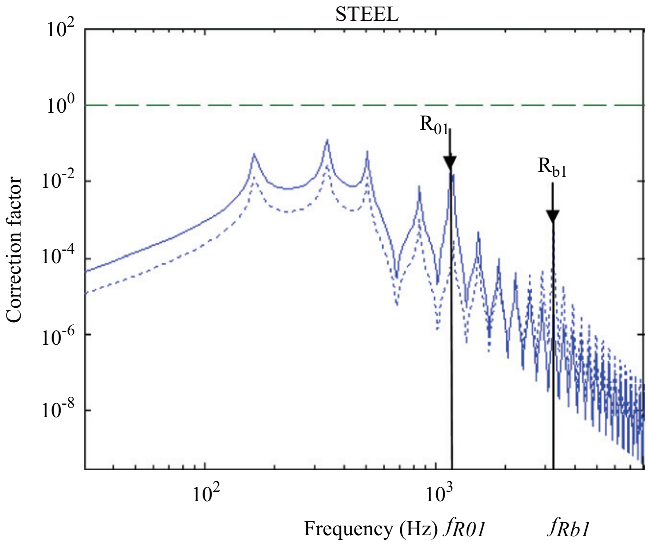

Fig. 6. The distorted (——— C_d) and non-distorted (...... C_n) correction factor of the acoustic input impedance induced by the wall vibration measured against frequency. The thickness of the shell is $h = 0.35$ mm and the material used is steel: its Young's modulus is $E = 210 \times 10^9\,\mathrm{N/m^2}$, its Poisson's ratio is $\sigma = 0.28$ and its density $\rho_S = 7800\,\mathrm{kg/m^3}$. C_n is altered by the eigenfrequency of the first breathing shell mode ($f_{\mathrm{Rb1}} = 3243$ Hz) which is greater than the peak in C_d which corresponds to the eigenfrequency of the first ovalling shell mode ($f_{\mathrm{Ro1}} = 1159$ Hz).

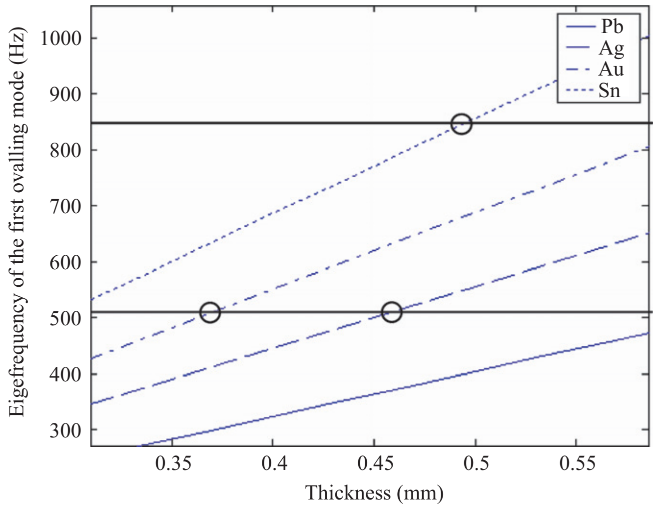

Fig. 7. The eigenfrequenies of the first ovalling shell mode against the shell thickness h for different shells made of four different materials (——— lead (Pb), – – – silver (Ag), –·–· gold (Au) and ...... tin (Sn)). The geometry of the shell is fixed at: length $l = 0.5$ m and radius $a = 14.25$ mm. Horizontal lines indicate the acoustic resonances frequencies of the plane mode equal to $(2n+1)c/4L$. Circles indicate matching conditions between shell and acoustic eigenfrequencies.

the non-distorted correction factor. The eigenfrequency of the first ovalling shell mode ($f_{\mathrm{Ro1}} = 1159$ Hz) can be observed as a maximum of the distorted correction factor.

In Fig. 6, it can be seen that f_{Ro1} is smaller than f_{Rb1}. In these conditions, the coupling of lower frequency modes (ovalling modes) with the air column can be produced, providing more important effects on the acoustic behaviour of the tube.

3.4. Study of configurations leading to important value of the correction factor

3.4.1. Influence of the material and shell thickness on the correction factor

For some materials, the eigenfrequency of the first ovalling mode can be sufficiently low to match the first acoustic eigenfrequencies. This configuration leads to a strong perturbation of the acoustic input impedance of the tube. Numerical tests have shown that this is the case for lead, silver, gold and tin. In Fig. 7, the eigenfrequency of the first ovalling shell mode is represented against the thickness of the different shells made from these materials. It can be seen that, in such cases, the mechanical resonance can be produced at frequencies close to the acoustic resonance of the tube. These resonances are indicated in Fig. 7. Intersection points indicated by circles provide the values of the shell thickness for which the eigenfrequency of the first ovalling mode matches with an acoustic eigenfrequency.

In the case of silver, the thickness of the shell can be adjusted in order to superpose the first mechanical resonance of the shell with the second acoustic resonance at 515.1 Hz. The thickness is found to be $h = 0.466$ mm as shown in Fig. 7. The correction factor and the acoustic input impedance of this silver shell are represented in Fig. 8a and b. Important changes in the first two acoustic resonances of the acoustic impedance due to wall vibrations in the distorted shell can be seen in both cases when compared with the non-vibrating shell reference. Thus, the acoustic behaviour of the shell is notably affected by the vibroacoustic coupling engendered by the distortion of the shell.

3.4.2. Influence of the distortion parameter on the correction factor

Provided that the distortion of the shell is mainly responsible for the significance of the fluid/shell coupling, an in-depth evaluation of this relationship is of interest. Fig. 9 shows the non-distorted correction factor corresponding to shells with different distortion factors ($\varepsilon = 0.05$, 0.25 and 0 that corresponds to a non-distorted shell). It can be seen that the greater the distortion, the greater the correction factor of the acoustic input impedance will be, and, as such, the wall vibration effect will be greater. For this shell, a distortion factor

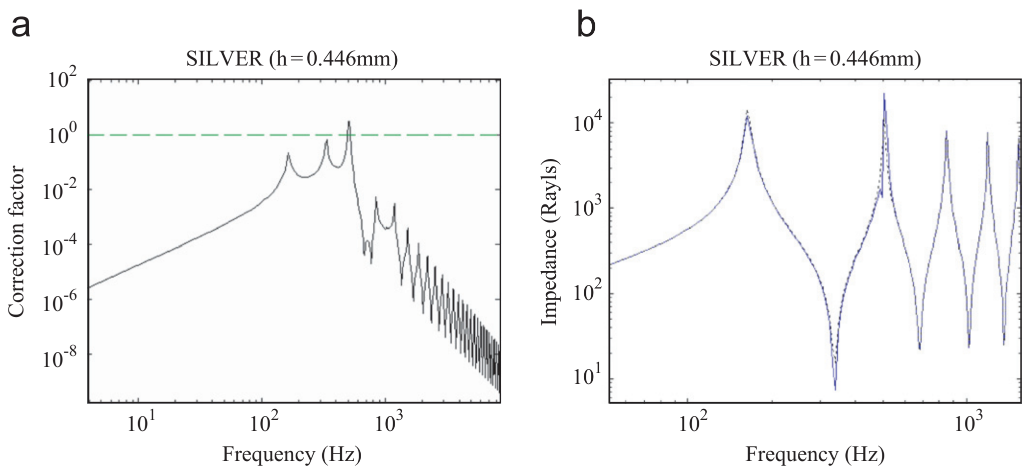

Fig. 8. (a) The correction factor and (b) the input acoustic impedance (——— Z^a) of a wall vibrating cylinder made of silver ($E = 30 \times 10^9\,\mathrm{N/m^2}$, its Poisson's ratio is $\sigma = 0.37$ and its density $\rho_S = 10{,}490\,\mathrm{kg/m^3}$). The reference of the acoustic input impedance of a rigid shell is represented (...... Z^r) in (b). The geometry of the shell is: length $l = 0.5\,\mathrm{m}$, radius $a = 14.25\,\mathrm{mm}$ and thickness $h = 0.466\,\mathrm{mm}$ and the distortion parameter is fixed at $\varepsilon = 0.05$. The eigenfrequency of the first ovalling mode (f_{b1}) is placed at the third acoustic resonances (f_3).

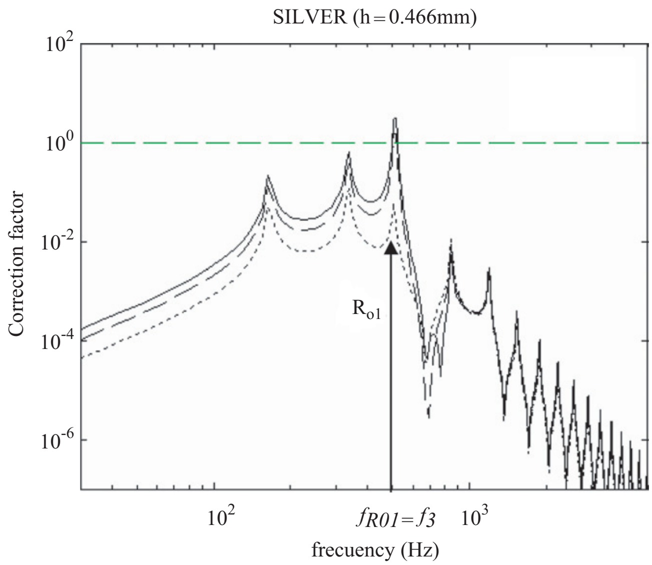

Fig. 9. The correction factor for four distorted shells, each made of silver each different from the other ($E = 30 \times 10^9\,\mathrm{N/m^2}$, $\sigma = 0.37$, $\rho_S = 10{,}490\,\mathrm{kg/m^3}$). The distortion factor of each shell is ——— $\varepsilon = 0.05$, —— $\varepsilon = 0.025$ and ...... $\varepsilon = 0$ (the latter is non-distorted). The geometry of the shell is such that the eigenfrequency of the first ovalling mode (f_{b1}) matches with the third acoustic resonances (f_3).

greater than $\varepsilon = 0.025$ provides a significant correction factor (greater than unity). However, it must be pointed out that these distortion factors are beyond the reaches of the validity of the vibroacoustic model hypothesis (limitations presented in Eqs. (13), (14) and (22)).

3.4.3. Influence of the structural damping coefficient on the correction factor

Although the distortion factor of the shell is very small, the wall vibration effect can be very important when the structural damping of the modes of the shell (η) is sufficiently small. In Fig. 10, the correction factor of three different distorted shells made of silver with different structural losses ($\eta = 0.1$, 0.01 and 0.001) have been represented. The distortion parameter is always $\varepsilon = 0.01$, that is, the distortion represents 1% of the

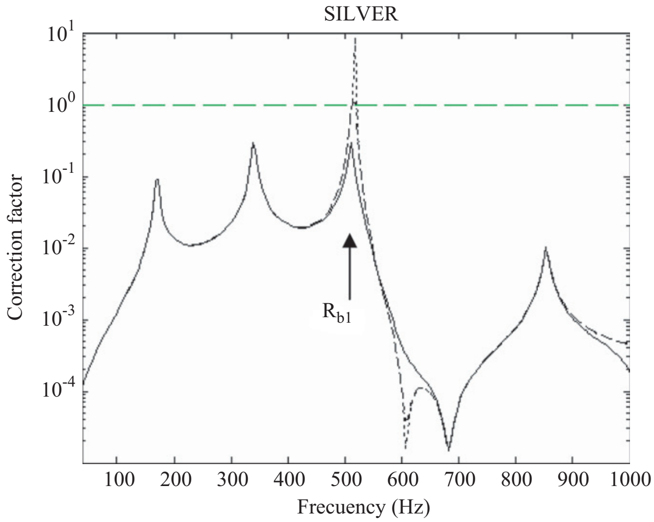

Fig. 10. The correction factor for three different distorted shells ($\varepsilon = 0.01$) each made of silver ($E = 30 \times 10^9\,\mathrm{N/m^2}$, $\rho_S = 10\,490\,\mathrm{kg/m^3}$ and $\sigma = 0.37$) with different structural damping coefficients (——— $\eta = 0.1$, – – – $\eta = 0.01$ and ...... $\eta = 0.001$). The eigenfrequency of the first ovalling mode (f_{Ro1}) is matched with the third acoustic resonances (f_3).

radius: 0.14 mm of distortion compared to 14.25 mm. Parameters E, σ, ρ_S and h have been selected to allow the eigenfrequency of the first ovalling mode to coincide with the third acoustic resonance of the tube. In Fig. 10, it can be observed that the curve corresponding to a shell having a material with structural losses of $\eta = 0.001$, greatly surpasses unity. In this case, the wall vibration effect is significant.

4. Conclusion

A vibroacoustic model of a simply supported distorted cylindrical shell has been developed and the influence of the distortion of the shell on the inner fluid/shell coupling has been quantified. It is shown that the shell distortion induces coupling between modes whose circumferential indices are different and the coupling coefficients between these modes can be predicted using the model. The influence of the wall vibration on the acoustic behaviour of a distorted tube can be understood as a correction of the acoustic matrix impedance which is called the "correction factor". The correction factor of the input acoustic impedance matrix of the distorted vibrating resonator was obtained as a sum of two contributions: the first C_n describes the interaction between the breathing modes and the plane acoustic mode; and, the second C_d describes the interaction between the ovalling modes and the plane acoustic mode. When considering slightly distorted shells, this second factor can be more important than the first. As a matter of fact, for some materials, the shell mechanical response is of such a nature that the eigenfrequency of the ovalling modes is sufficiently small to alter the first peaks of the acoustic input impedance of the tube. A numerical application permits the presentation of the interaction between the plane acoustic mode and the first ovalling mode when the distortion of the shell is small. Previous experimental results obtained with slightly distorted organ pipes can be interpreted using the proposed model. The validity of the results is limited by the hypothesis of the model: the distortion of the shell must be very small. This model confronts a well-known problem within the field of wind instruments: the wall vibration effect. Simulations in the time domain of distorted tubes could provide additional information about the fluid/shell coupling through the oscillation regime and vibrating distorted pipes.

Acknowledgements

The authors would like to thank Joel Gilbert for his helpful comments and the discussions.

Appendix A. Matrix notations

The matrix formulation of the problem is useful for the description of the multimodal approach. Thus, vectors

$$\mathbf{A}_m = \begin{bmatrix} A_{(m,1,s)} \\ \vdots \\ A_{(m,Q,s)} \end{bmatrix}, \tag{A.1}$$

$$\mathbf{P}_m = \begin{bmatrix} P_{(m,0,s)} = \langle p|\Psi_{(m,0,s)} \rangle \\ \vdots \\ P_{(m,N,s)} = \langle p|\Psi_{(m,N,s)} \rangle \end{bmatrix}, \tag{A.2}$$

$$\mathbf{V}_m = \begin{bmatrix} V_{(m,0,s)} = \langle V_{S_0}|\Psi_{(m,0,s)} \rangle \\ \vdots \\ V_{(m,N,s)} = \langle V_{S_0}|\Psi_{(m,N,s)} \rangle \end{bmatrix}, \tag{A.3}$$

describe the unknown modal amplitudes for a given circumferential index m. For each m, the mechanical basis is truncated to the Q modes and the acoustic basis is reduced to the N modes. Grouping these amplitude vectors as

$$\mathbf{A} = \begin{bmatrix} \mathbf{A}_1 \\ \vdots \\ \mathbf{A}_m \\ \vdots \\ \mathbf{A}_M \end{bmatrix}, \tag{A.4}$$

$$\mathbf{P} = \begin{bmatrix} \mathbf{P}_1 \\ \vdots \\ \mathbf{P}_m \\ \vdots \\ \mathbf{P}_M \end{bmatrix}, \tag{A.5}$$

$$\mathbf{V} = \begin{bmatrix} \mathbf{V}_1 \\ \vdots \\ \mathbf{V}_m \\ \vdots \\ \mathbf{V}_M \end{bmatrix}, \tag{A.6}$$

we obtain modal amplitude vectors for the shell displacement $\mathbf{A}$, the acoustic pressure $\mathbf{P}$ and the velocity $\mathbf{V}$.

The rigid impedance matrix $\mathbf{Z}^r$ is a diagonal matrix that corresponds to the input acoustic impedance of the cylinder with rigid walls, and therefore, it does not take the wall vibration effect into consideration:

$$\mathbf{Z}^r = \begin{bmatrix} Z^r_{(0,0,0),(0,0,0)} & 0 & 0 \\ 0 & \ddots & 0 \\ 0 & 0 & Z^r_{(m,n,s),(m',n',s')} \end{bmatrix}. \tag{A.7}$$

The boldtype of $\mathbf{Z}^r$ represents the matrix character of the rigid impedance and each element written in italics represents a scalar. Matrix $\mathbf{M}$ describes the mechanical behaviour of the shell:

$$\mathbf{M} = \begin{bmatrix} M_{(0,1,0),(0,1,1)} & 0 & 0 \\ 0 & \ddots & 0 \\ 0 & 0 & M_{(m,q,s),(m',q',s')} \end{bmatrix}. \tag{A.8}$$

Matrices $\mathbf{Q}$ and $\mathbf{E}$ contain the vibroacoustic coupling terms:

$$\mathbf{E} = \begin{bmatrix} E_{(0,1,0),(0,0,0)} & \cdots & E_{(0,1,0),(m,n,s)} \\ \vdots & \ddots & \vdots \\ E_{(m',q',s'),(0,0,0)} & \cdots & E_{(m',q',s'),(m,n,s)} \end{bmatrix} \tag{A.9}$$

and

$$\mathbf{Q} = \begin{bmatrix} Q_{(0,0,0),(0,1,0)} & \cdots & Q_{(0,0,0),(m',q',s')} \\ \vdots & \ddots & \vdots \\ Q_{(m,n,s),(0,1,0)} & \cdots & Q_{(m,n,s),(m',q,s')} \end{bmatrix}. \tag{A.10}$$

The product of $\mathbf{Q}\ \mathbf{M}^{-1}\ \mathbf{E}$ provides the correction factor wich is not a diagonal matrix due to the fact that neither $\mathbf{Q}$ nor $\mathbf{E}$ are diagonal. The off-diagonal terms of matrix $\mathbf{C}$ represent the coupling between the shell modes and acoustic modes.

Appendix B. Matrix notations for the truncation considered

In order to evaluate the wall vibration effect on the acoustic behaviour of the shell, the simplest modal truncation resulting in the effect of shell distortion has been considered. Thus, m and m' vary from 0 to 2, s and s' vary from 0 to 1 and indices q and n take the first value of the truncation ($q = 1$ and $n = 0$). This implies that the coupling between six acoustic modes and six shell modes is taken into account. For this truncation, matrices $\mathbf{Q}_{\alpha\mu'} = \mathbf{Q}_{(m,n,s)(m',q',s')}$, $\mathbf{M}_{\mu\mu'} = \mathbf{M}_{(m,q,s)(m'q',s')}$ and $\mathbf{E}_{\mu'\alpha} = \mathbf{E}_{(m',q',s')(m,n,s)}$ can be represented as (6×6) matrices:

$$\mathbf{Q}_{\alpha\mu'} = \begin{pmatrix} 0 & 0 & 0 & 0 & 0 & 0 \\ 0 & Q_{(0,0,1)(0,1,1)} & 0 & 0 & 0 & Q_{(0,0,1)(2,1,1)} \\ 0 & 0 & Q_{(1,0,0)(1,1,0)} & 0 & 0 & 0 \\ 0 & 0 & 0 & Q_{(1,0,1)(1,1,1)} & 0 & 0 \\ 0 & 0 & 0 & 0 & Q_{(2,0,0)(2,1,0)} & 0 \\ 0 & Q_{(2,0,1)(0,1,1)} & 0 & 0 & 0 & Q_{(2,0,1)(2,1,1)} \end{pmatrix} \tag{B.1}$$

and

$$\mathbf{M}_{\mu\mu'} = \begin{pmatrix} M_{(0,1,0)(0,1,0)} & 0 & 0 & 0 & 0 & 0 \\ 0 & M_{(0,1,1)(0,1,1)} & 0 & 0 & 0 & 0 \\ 0 & 0 & M_{(1,1,0)(1,1,0)} & 0 & 0 & 0 \\ 0 & 0 & 0 & M_{(1,1,1)(1,1,1)} & 0 & 0 \\ 0 & 0 & 0 & 0 & M_{(2,1,0)(2,1,0)} & 0 \\ 0 & 0 & 0 & 0 & 0 & M_{(2,1,1)(2,1,1)} \end{pmatrix}, \tag{B.2}$$

$$\mathbf{E}_{\mu'\alpha} = \begin{pmatrix} 0 & 0 & 0 & 0 & 0 & 0 \\ 0 & E_{(0,1,1)(0,0,1)} & 0 & 0 & 0 & E_{(0,1,1)(2,0,1)} \\ 0 & 0 & E_{(1,1,0)(1,0,0)} & 0 & 0 & 0 \\ 0 & 0 & 0 & E_{(1,1,1)(1,0,1)} & 0 & 0 \\ 0 & 0 & 0 & 0 & E_{(2,1,0)(2,0,0)} & 0 \\ 0 & E_{(2,1,1)(0,0,1)} & 0 & 0 & 0 & E_{(2,1,1)(2,0,1)} \end{pmatrix}, \tag{B.3}$$

where

$$Q_{(0,0,1)(0,1,1)} = -\frac{\rho\omega^2}{k}\frac{\pi\sqrt{\pi}}{al}\frac{\tan(kl)}{k^2 - (\pi/l)^2}(2-\varepsilon),$$

$$Q_{(1,0,0)(1,1,0)} = Q_{(1,0,1)(1,1,1)} = -\frac{\rho\omega^2}{l}\frac{\pi\sqrt{2\pi}}{\sqrt{(k_{10}a)^2-1}}\frac{\tan(k_{10}l)}{k_{10}^2 - (\pi/l)^2}(1-\varepsilon),$$

$$Q_{(2,0,0)(2,1,0)} = Q_{(2,0,1)(2,1,1)} = -\frac{\rho\omega^2}{l}\frac{\pi\sqrt{2\pi}}{\sqrt{(k_{20}a)^2-1}}\frac{\tan(k_{20}l)}{k_{20}^2 - (\pi/l)^2}(1-\varepsilon),$$

$$Q_{(0,0,1)(2,1,1)} = -\frac{\rho\omega^2}{k}\frac{\pi\sqrt{\pi}}{al}\frac{\tan(kl)}{k^2 - (\pi/l)^2}2\varepsilon,$$

$$Q_{(2,0,1)(0,1,1)} = -\frac{\rho\omega^2}{l}\frac{\pi\sqrt{2\pi}}{\sqrt{(k_{20}a)^2-1}}\frac{\tan(k_{20}l)}{k_{20}^2 - (\pi/l)^2}2\varepsilon$$

and where

$$M_{(m,n,s),(m,n,s)} = m_{(m,n,s)}(\omega^2 - \omega^2_{(m,n,s)}(1 - \mathrm{j}\eta_{(m,n,s)}))$$

and finally

$$E_{(0,1,1)(0,0,1)} = \frac{\mathrm{j}\rho\omega}{k}\frac{\pi\sqrt{\pi}}{al}\frac{\tan(kl)}{k^2 - (\pi/l)^2}(2-\varepsilon),$$

$$E_{(1,1,0)(1,0,0)} = E_{(1,1,1)(1,0,1)} = \frac{\mathrm{j}\rho\omega}{l}\frac{\pi\sqrt{2\pi}}{\sqrt{(k_{10}a)^2-1}}\frac{\tan(k_{10}l)}{k_{10}^2 - (\pi/l)^2}(1-\varepsilon),$$

$$E_{(2,1,0)(2,0,0)} = E_{(2,1,1)(2,0,1)} = \frac{\mathrm{j}\rho\omega}{l}\frac{\pi\sqrt{2\pi}}{\sqrt{(k_{20}a)^2-1}}\frac{\tan(k_{20}l)}{k_{20}^2 - (\pi/l)^2}(1-\varepsilon),$$

$$E_{(2,1,1)(0,0,1)} = \frac{j\rho\omega}{k}\frac{\pi\sqrt{\pi}}{al}\frac{\tan(kl)}{k^2 - (\pi/l)^2}2\varepsilon,$$

$$E_{(0,1,1)(2,0,1)} = \frac{j\rho\omega}{l}\frac{\pi\sqrt{2\pi}}{\sqrt{(k_{20}a)^2 - 1}}\frac{\tan(k_{20}l)}{k_{20}^2 - (\pi/l)^2}\,2\varepsilon.$$

The impedance correction ($Z = Z^r + Z^c$) for this truncation can be evaluated using the product of matrices (B.1)–(B.3) as

$$\mathbf{Z}^c_{\alpha\alpha'''} = \mathbf{Q}_{\alpha\mu'}\mathbf{M}^{-1}_{\mu'\mu''}\mathbf{E}_{\mu''\alpha'''},$$

$$\mathbf{Z}^c_{(m,n,s)(m''',n''',s''')} = \mathbf{Q}_{(m,n,s)(m',q',s')}\mathbf{M}^{-1}_{(m',q',s')(m'',q'',s'')}\mathbf{E}_{(m'',q'',s'')(m''',n''',s''')},$$

$$\mathbf{Z}^c_{\alpha\alpha'} = \begin{pmatrix} 0 & 0 & 0 & 0 & 0 & 0 \\ 0 & Z^c_{(0,0,1)(0,0,1)} & 0 & 0 & 0 & Z^c_{(0,0,1)(2,0,1)} \\ 0 & 0 & Z^c_{(1,0,0)(1,0,0)} & 0 & 0 & 0 \\ 0 & 0 & 0 & Z^c_{(1,0,1)(1,0,1)} & 0 & 0 \\ 0 & 0 & 0 & 0 & Z^c_{(2,0,0)(2,0,0)} & 0 \\ 0 & Z^c_{(2,0,1)(0,0,1)} & 0 & 0 & 0 & Z^c_{(2,0,1)(2,0,1)} \end{pmatrix}, \tag{B.4}$$

where

$$Z^c_{(0,0,1)(0,01)} = Q_{(0,0,1)(0,1,1)}M^{-1}_{(0,1,1)(0,1,1)}E_{(0,1,1)(0,0,1)} + Q_{(0,0,1)(2,1,1)}M^{-1}_{(2,1,1)(2,1,1)}E_{(2,1,1)(0,0,1)},$$

$$Z^c_{(0,0,1)(2,0,1)} = Q_{(0,0,1)(0,1,1)}M^{-1}_{(0,1,1)(0,1,1)}E_{(0,1,1)(2,0,1)} + Q_{(0,0,1)(2,1,1)}M^{-1}_{(2,1,1)(2,1,1)}E_{(2,1,1)(2,0,1)},$$

$$Z^c_{(1,0,0)(1,0,0)} = Q_{(1,0,0)(1,1,0)}M^{-1}_{(1,1,0)(1,1,0)}E_{(1,1,0)(1,0,0)},$$

$$Z^c_{(1,0,1)(1,0,1)} = Q_{(1,0,1)(1,1,1)}M^{-1}_{(1,1,1)(1,1,1)}E_{(1,1,1)(1,0,1)},$$

$$Z^c_{(2,0,0)(2,0,0)} = Q_{(2,0,0)(2,1,0)}M^{-1}_{(2,1,0)(2,1,0)}E_{(2,1,0)(2,0,0)},$$

$$Z^c_{(2,0,1)(0,0,1)} = Q_{(2,1,1)(0,1,1)}M^{-1}_{(0,1,1)(0,1,1)}E_{(0,1,1)(0,0,1)} + Q_{(2,0,1)(2,1,1)}M^{-1}_{(2,1,1)(2,1,1)}E_{(2,1,1)(0,0,1)},$$

$$Z^c_{(2,0,1)(2,0,1)} = Q_{(2,0,1)(0,1,1)}M^{-1}_{(0,1,1)(0,1,1)}E_{(0,1,1)(2,0,1)} + Q_{(2,0,1)(2,1,1)}M^{-1}_{(2,1,1)(2,1,1)}E_{(2,1,1)(2,0,1)}. \tag{B.5}$$

References

[1] R. Smith, The effect of material in brass instruments; a review, *Proceedings of the Institute of Acoustics* 8 (1) (1986) 91–96.

[2] F. Gautier, Tahani, Vibroacoustic behavior of a simplified musical wind instrument, *Journal of Sound and Vibration* 213 (1998) 107–125.

[3] R. Picó, F. Gautier, J. Redondo, Acoustic input impedance of a vibrating cylindrical tube, *Journal of Sound and Vibration*, in press, doi:10.1016/j.jsv.2006.10.030.

[4] B. Gazengel, J. Gilbert, N. Amir, Time domain simulation of single reed wind instrument. From the measured input impedance to the synthesis signal. Where are the tramps?, *Acustica* 3 (1995) 445–472.

[5] R. Picó Vila, J. Gilbert, F. Gautier, Study of the input acoustic impedance of a vibrating cylindrical shell: consequences on clarinet-like instrument. *Proceedings of the Seventh CFA/DAGA*, Strasbourg, France, 22–25 March 2004.

[6] A.W. Leissa, *Vibrations of Shells*, NASA, Washington, DC, 1973.

[7] J.-Y. Elegoet, *Mémoire de DEA, INSA de Lyon*, Vibrations des coques distordues, 1993 (in French).

[8] L. Maxit, *Mémoire de DEA, INSA de Lyon*, Etude du rayonnement et de la transparence des coques distordues, 1995 (in French).

[9] B. Laulagnet, Rayonnement acoustique extérieur des coques infinies présentant des petits défauts de circularité, *Proceedings of the Institute of Acoustics*, Vol. 15, Part 3, 1993, pp. 731–738.
[10] J.L. Guyader, B. Laulagnet, Structural Acoustic Radiation prediction: expanding the vibratory response on a functional basis, *Applied Acoustics* 43 (1994) 247–269.
[11] E.C. Pestel, F.A. Leckie, *Matrix methods in elastomechanics*, Mc Graw-Hill, New York, 1963.
[12] Z. Wang, A.N. Norris, Waves in cylindrical shells with circumferential submembers: a matrix approach, *Journal of Sound and Vibration* 181 (3) (1995) 457–484.
[13] M.-H. Moulet, Caractérisation des jonctions en mécanque vibratoire, PhD Thesis, Université du Maine, Le Mans, France, 2003 (in French).
[14] G. Yamada, T. Irie, Y. Tagwa, Free vibration of non-circular cylindrical shells with variable circumferential profile, *Journal of Sound and Vibration* 95 (1) (1984) 117–126.
[15] T. Irie, G. Yamada, Y. Kobayashi, Free vibrations of non-circular cylindrical shells with longitudinal interior partitions, *Journal of Sound and Vibration* 96 (1) (1984) 133–142.
[16] K. Shirakawa, M. Morita, Vibration and buckling of cylinders with elliptical cross section, *Journal of Sound and Vibration* 84 (1) (1982) 121–131.
[17] S.N. Yousri, F.J. Fahy, Distorted cylindrical shell response to internal acoustic excitation below the cut-off frequency, *Journal of Sound and Vibration* 52 (3) (1977) 441–452.
[18] M. Bruneau, *Manuel d'Acoustique Fondamentale*, Editions Hermes, Paris, 1998 (in French).
[19] P.M. Morse, K.U. Ingard, *Theoretical Acoustics*, Princeton University Press, Princeton, 1986.
[20] F. Gautier, Contribution à l'étude du comportement vibroacoustique des instruments de musique à vent, PhD thesis, Université du Maine, Le Mans, France, 1997 (in French).
[21] K. Forsberg, Influence of boundary conditions on the modal characteristics of thin cylindrical shells, *AIAA* 2 (12) (1964) 2150–2157.